

Progress on Constraining the Strange Quark Contribution to the Proton Axial Form Factor

**S.F. Pate¹, V. Papavassiliou¹, J.P. Schaub¹, D.P. Trujillo¹,
M.V. Ivanov², M.B. Barbaro^{3,4}, C. Giusti⁵**

¹New Mexico State University, Las Cruces, New Mexico, 88003, USA

²Institute for Nuclear Research and Nuclear Energy,
Bulgarian Academy of Sciences, Sofia 1784, Bulgaria

³Università degli Studi di Torino, Turin, Italy

⁴Istituto Nazionale di Fisica Nucleare, Sezione di Torino, Italy

⁵Istituto Nazionale di Fisica Nucleare, Sezione di Pavia, Italy

Abstract. We report on a global fit of neutral-current elastic (NCE) neutrino-scattering data and parity-violating electron-scattering (PVES) data with the goal of determining the strange quark contribution to the vector and axial form factors of the proton. Knowledge of the strangeness contribution to the axial form factor, $G_A^s(Q^2)$, at low Q^2 will reveal the strange quark contribution to the nucleon spin, as $G_A^s(Q^2 = 0) = \Delta s$. Previous fits [1, 2] of this form included data from a variety of PVES experiments (PVA4, HAPPEX, G0, SAMPLE) and the NCE neutrino and anti-neutrino data from BNL E734. These fits did not constrain $G_A^s(Q^2)$ at low Q^2 very well because there was no NCE data for $Q^2 < 0.45 \text{ GeV}^2$. Our new fit includes for the first time MiniBooNE NCE data from both neutrino and anti-neutrino scattering; this experiment used a hydro-carbon target and so a model of the neutrino interaction with the carbon nucleus was required. Three different nuclear models have been employed; a relativistic Fermi gas (RFG) model, the SuperScaling Approximation (SuSA) model, and a spectral function (SF) model [3]. We find a tremendous improvement in the constraint of $G_A^s(Q^2)$ at low Q^2 compared to previous work, although more data is needed from NCE measurements that focus on exclusive single-proton final states, for example from MicroBooNE [4]. This work has been published in Physical Review D [5].

1 Physics Motivation

The axial form factor of the proton $G_A(Q^2)$ is the leading contributor to the interactions of neutrinos with matter, just as the electric and magnetic form factors are the leading contributors to the interactions of electrons with matter. It may be written as a sum over contributions from individual quarks.

$$G_A(Q^2) = \frac{1}{2} [-G_A^u(Q^2) + G_A^d(Q^2) + G_A^s(Q^2)] .$$

The up-down part,

$$G_A^{CC}(Q^2) = -G_A^u(Q^2) + G_A^d(Q^2),$$

is very well-known from decades of study of charged-current (CC) interactions, for example $\nu_\mu + n \rightarrow \mu + p$ and $n \rightarrow p + e^- + \bar{\nu}_e$. The strange part,

$$G_A^s(Q^2),$$

by contrast is only directly accessible via neutral-current (NC) interactions, for example $\nu + p \rightarrow \nu + p$, for which there is very little data compared to CC interactions. We have still only limited information about $G_A^s(Q^2)$.

In practical models of neutrino interactions, it is necessary to create some form for $G_A^s(Q^2)$. Two common ingredients are found in these models:

- It is assumed that the Q^2 -dependence of $G_A^s(Q^2)$ is the same as $G_A^{CC}(Q^2)$, that is a dipole form using an “axial mass” M_A taken from studies of CC data. But there is no physics underlying this assumption.
- The value of $G_A^s(Q^2)$ at $Q^2 = 0$ is the strange quark contribution to the proton spin, usually called Δs . A value for Δs from polarized deep-inelastic scattering data is then taken for use in the model. However, there is no agreed upon value for Δs from pDIS data; values range anywhere from 0.0 to -0.2. This results in a big uncertainty in the modeling.

Our goal here is to determine both the Q^2 -dependence of $G_A^s(Q^2)$ and the value of Δs directly from elastic electron and neutrino scattering data.

There is quite a broad physics interest in the value of Δs . A few examples:

- Some searches for dark-matter particles depend upon a knowledge of Δs [6].
- Lattice QCD calculates Δs to be very small, e.g. $\Delta s = -0.031(17)$ [7] and $\Delta s = -0.024(15)$ [8]. This requires experimental verification.
- Simulations of supernovae are sensitive to the value of Δs [9].
- Atomic parity-violating measurements on hydrogen are sensitive to Δs [10].

Our approach will be to determine simultaneously the strange quark contribution to the electric, magnetic and axial form factors ($G_E^s(Q^2)$, $G_M^s(Q^2)$, and $G_A^s(Q^2)$ respectively) by combining data from neutrino neutral current elastic scattering (NCES) and parity-violating electron scattering (PVES). This was first done in [11] by combining BNL E734 NCES data with HAPPEX PVES data at $Q^2 = 0.477 \text{ GeV}^2$. This analysis was expanded [1] to include points in the range $0.55 < Q^2 < 1.05 \text{ GeV}^2$ when the G0 PVES data became available. Other analyses focused only on the PVES data and extracted only $G_E^s(Q^2)$

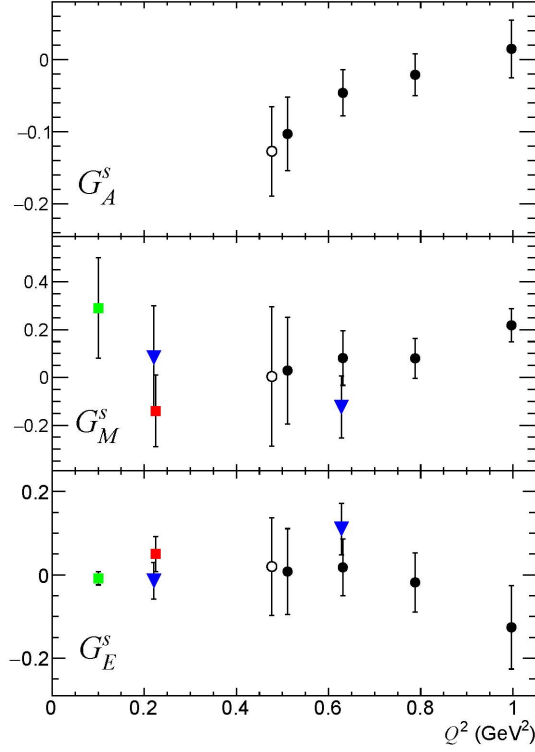


Figure 1. Independent determinations of the strangeness form factors of the nucleon using subsets of existing experimental data: Liu et al. (green squares) [12]; Androić et al. (blue triangles) [13]; Baunack et al. (red squares) [14]; Pate et al. (open circles use HAPPEX and E734 data, and closed circles use G0-Forward and E734 data) [1]. This selection of results is representative and not intended to be exhaustive.

and $G_M^s(Q^2)$. The results of these various analyses are summarized in Figure 1. We observe that the strange quark contribution to the electric and magnetic form factors, $G_E^s(Q^2)$ and $G_M^s(Q^2)$, are consistent with zero throughout the range $0.0 < Q^2 < 1.1 \text{ GeV}^2$. On the other hand, $G_A^s(Q^2)$ has a definite Q^2 -dependence, trending negative with decreasing Q^2 .

2 Description of the Method

To make progress with the determination of these form factors, we need to transition from determining the form factors at local values of Q^2 to a global fit that uses all of the data points. This means we need parametrized functional forms for $G_E^s(Q^2)$, $G_M^s(Q^2)$, and $G_A^s(Q^2)$. Based on the results seen in Figure 1, we

have chosen very simple, zeroth-order forms for $G_E^s(Q^2)$ and $G_M^s(Q^2)$.

$$G_E^s(Q^2) = \rho_s \tau, \quad \tau = Q^2/4M^2, \quad G_M^s(Q^2) = \mu_s,$$

where ρ_s is the strangeness radius, and μ_s is the strangeness contribution to the magnetic moment. By contrast, the data on G_A^s shows a definite Q^2 -dependence, and for this form factor we have chosen to use two different 3-parameter models.

- The Modified-Dipole Model: The expression used for the strangeness axial form factor is

$$G_A^s = \frac{\Delta s + S_A Q^2}{(1 + Q^2/\Lambda_A^2)^2},$$

where Δs is the strange quark contribution to the proton spin, and S_A and Λ_A are parameters describing the Q^2 -dependence of G_A^s . This shape is referred to as a “modified-dipole” because of its similarity to the usual dipole shapes used to model other form factors.

- The z -Expansion Model: The modified-dipole model comes with a bias with respect to the Q^2 -dependence of G_A^s . The “ z -expansion” technique [15, 16] allows for a bias-free model because it is simply a power series, and the fit seeks to determine the coefficients of the series. The power series is of the form

$$G_A^s(Q^2) = \sum_{k=0}^{\infty} a_k [z(Q^2)]^k,$$

where Q^2 has been mapped onto the variable z as follows:

$$z(Q^2, t_{\text{cut}}, t_0) = \frac{\sqrt{t_{\text{cut}} + Q^2} - \sqrt{t_{\text{cut}} - t_0}}{\sqrt{t_{\text{cut}} + Q^2} + \sqrt{t_{\text{cut}} - t_0}}.$$

Note that $|z| < 1$. The parameter t_{cut} is determined by the threshold of the relevant current, which in the case of the isoscalar axial current is $t_{\text{cut}} = (4m_\pi)^2$. (As an example, the lightest decay mode of the $f_1(1285)$ meson, with $I^G(J^{PC}) = 0^+(1^{++})$, is four pions.) The parameter t_0 is arbitrary, and can be adjusted to make the convergence of the series more rapid, but we have chosen simply to use $t_0 = 0$; this has the consequence that $a_0 = \Delta s$. Of course it is necessary to cut off the sum over k , and we have limited it to $k_{\text{max}} = 6$. This would imply seven parameters for the description of G_A^s . However, due to the fact that the form factor should behave like $1/Q^4$ at large values of Q^2 , we have the following four conditions:

$$\left. \frac{d^n}{dz^n} G_A^s \right|_{z=1} = 0 \quad n = 0, 1, 2, 3.$$

This allows us to reduce the number of independent parameters from seven down to three: a_0 , a_1 , and a_2 .

Progress on Constraining the Strange Quark Contribution to ...

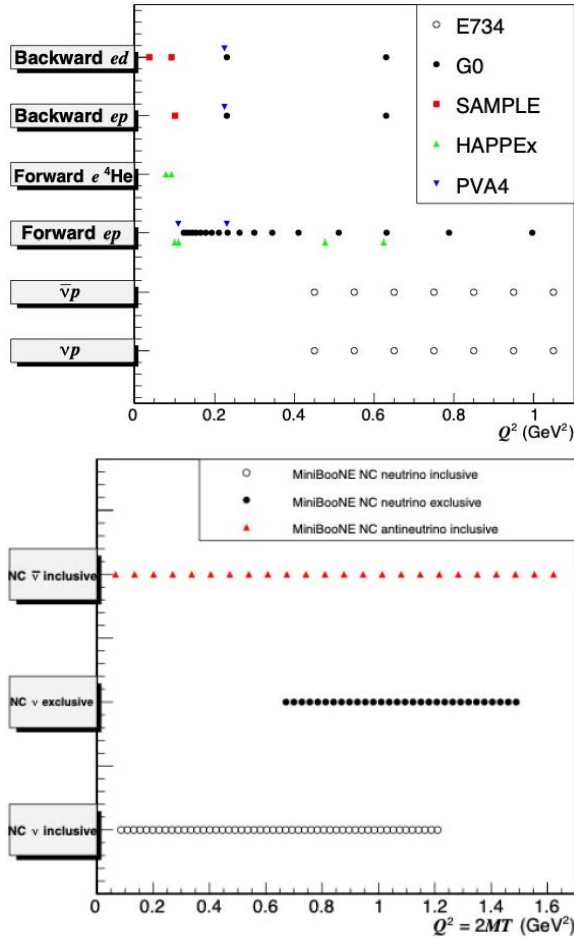


Figure 2. NCES and PVES data available for this analysis technique. We use MiniBooNE data in the range $0.1 < Q^2 < 1.1$ GeV²; there are then 128 data points in total.

Figure 2 illustrates the wide range of neutrino-scattering and electron-scattering data we will use in our analysis. In order to incorporate the MiniBooNE experiment, which used a hydrocarbon-based target/detector system, a model was needed for the neutrino-carbon interaction. We used three such models:

- Relativistic Fermi Gas (RFG): The carbon nucleus is described by a Fermi momentum k_F based on electron scattering data; the nucleons are plane waves constrained by the Pauli principle.
- SuperScaling Approximation (SuSA): Scaling behavior of (e, e') data are used to predict NC and CC neutrino-scattering cross sections.

- Spectral Function (SF): A spectral function $S(p, \mathcal{E})$ based on (e, e') data has been used to better describe single-nucleon removal.

Using the three nuclear models for carbon, and the two models for the strangeness form factors, we performed 6 distinct fits. In each fit, the five form factor parameters were varied to find the minimum χ^2 , and the behavior of the χ^2 near the minimum was used to determine the uncertainties in the parameters. The complete results are described in great detail in our publication [5]. In these proceedings we will simply illustrate in Figure 3 the effect of adding the MiniBooNE data to this analysis. It is seen that the constraint on the low- Q^2 behavior of $G_A^s(Q^2)$ is greatly improved by the introduction of the MiniBooNE data, while there is little change to the other form factors $G_E^s(Q^2)$ and $G_M^s(Q^2)$.

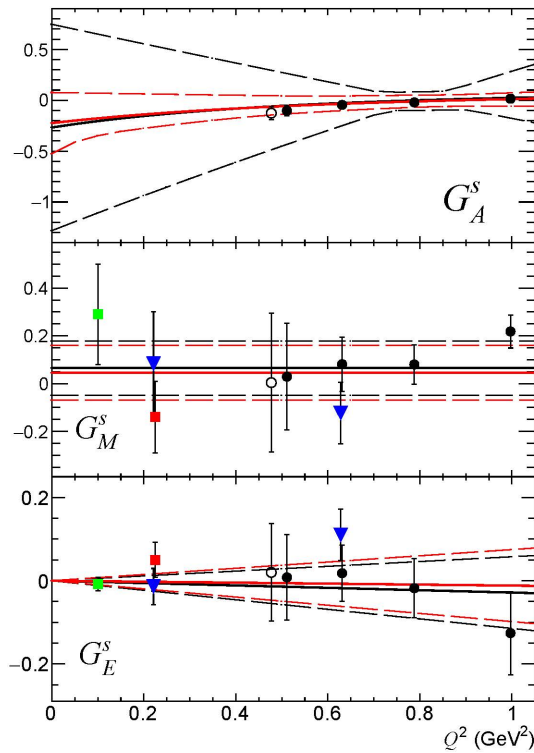


Figure 3. An illustration of the effect of the introduction of the MiniBooNE neutral current data into our global fit. The data points are the same as in Fig. 1. The black solid line is the central value for the modified-dipole fit not using the MiniBooNE data. The red solid line includes the MiniBooNE data using the spectral function nuclear model. The dashed lines represent the 70% confidence limit for each fit. As mentioned in the text, the vector form factors fit is only slightly affected by the introduction of the MiniBooNE data, while the constraints on the axial form factor are greatly improved.

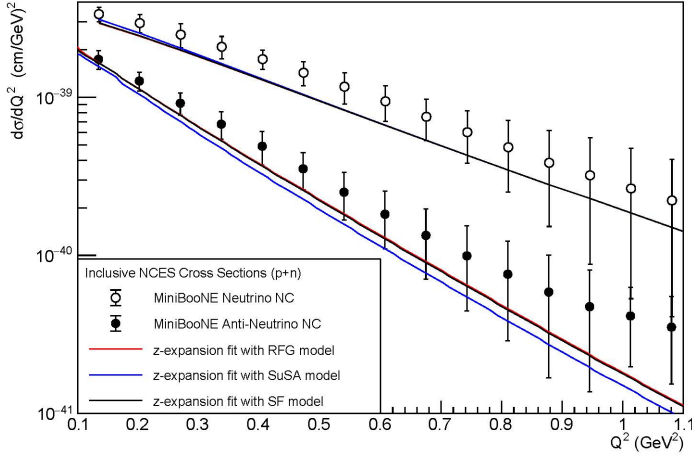


Figure 4. Comparison between our fits and the NC scattering data from MiniBooNE [17, 18], showing the cross sections from both the neutrino and antineutrino measurements. All three fits shown use the z -expansion model for G_A^s . The red line shows the results of the fit using the RFG nuclear model, the blue line shows the result using the SuSA nuclear model, and the black line is with the SF nuclear model. In all three cases the results for RFG (red) and SF (black) are very similar to each other and the lines almost overlap. Fit results using instead the modified-dipole model for G_A^s produce very similar results to those shown here.

In Figure 4 is an illustration of the quality of our calculations for the MiniBooNE cross sections, illustrating all three nuclear models; the z -expansion model is used for G_A^s . We tend to under predict the cross section in the region $0.3 - 0.6 \text{ GeV}^2$. An important ingredient, which is missing in the present models, is the contribution of two-body currents, which can lead to the excitation of $2p2h$ states. These contributions are not quasi-elastic, but they do contribute to the experimental signal represented in Fig. 4 and should be included in the calculation. In principle two-body currents could affect not only the cross sections but also the p/n ratios because of the isospin dependence of the current operator. However, while several calculations are now available for the $2p2h$ contribution to CC reactions, the corresponding calculations for NC scattering are very rare.

3 Conclusion

We have performed a global fit of parity-violating electron-scattering data from the HAPPEX, SAMPLE, G0 and PVA4 experiments and of neutral-current elastic scattering data from the BNL E734 and Fermilab MiniBooNE experiments, a total of 128 data points in the momentum transfer range $0.1 < Q^2 < 1.1 \text{ GeV}^2$, using two models for the strangeness form factors G_E^s , G_M^s , and G_A^s , and using three nuclear models to describe the interaction of neutrinos with the hydrocar-

bon target used in MiniBooNE. Our fits are in very good agreement with this collection of data, with $\chi^2/\text{ndf} \approx 1.1\text{-}1.2$ for all fits.

Depending on the model, we show a slightly negative value of the strangeness radius ρ_s but also consistent with zero, and a slightly positive value for the strangeness magnetic moment μ_s also consistent with zero; we note this outcome is slightly at odds with other workers, for example Ref. [19], who do not include neutrino NC scattering data into their fitting data set. To quantify our conclusion that ρ_s and μ_s are consistent with zero, we have taken $\rho_s = 0$ and $\mu_s = 0$ to be null hypotheses and then used our fit results for these quantities to calculate a corresponding p-value for each. For the null hypothesis $\rho_s = 0$ we find a p-value of 0.83; for the null hypothesis $\mu_s = 0$ we find a p-value of 0.42. These large p-values do not recommend a rejection of either of these null hypotheses.

The inclusion of the MiniBooNE neutral current data into the dataset has greatly improved the constraints on the strangeness axial form factor G_A^s , but still we cannot report a definite value for Δs on the basis of these fits. We can expect that a more refined model including two-body currents (which is currently not available but can hopefully become available in the future) would give a better description of the experimental NC cross section and might be helpful for an improved determination of the strange axial form factor, but presumably it should not change the main finding of our paper that the inclusion of the MiniBooNE neutral current data into the dataset greatly improves the constraints on G_A^s . Primarily, exclusive NCES data from proton interactions at low Q^2 are still needed for a complete determination of G_A^s , and we look forward to that data from MicroBooNE [4] in the near future.

Acknowledgements

We are grateful to the following funding agencies: US Department of Energy, Office of Science, Medium Energy Nuclear Physics Program, Grant DE-FG02-94ER40847; Bulgarian National Science Fund under Contract No. KP-06-N38/1; Istituto Nazionale di Fisica Nucleare under the National Project “NUCSYS”; University of Turin local research funds BARM-RILO-22. SFP is grateful for sabbatical support from both the Universities Research Association Visiting Scholars Program and the Los Alamos National Laboratory during 2022. We are also grateful to R. Dharmapalan for assistance in the interpretation of the MiniBooNE antineutrino NC data release.

References

- [1] S.F. Pate, D.W. McKee, V. Papavassiliou, *Phys. Rev. C* **78** (2008) 015207.
- [2] S. Pate, D. Trujillo, *EPJ Web Conf.* **66** (2014) 06018.
- [3] C. Giusti, M.V. Ivanov, *J. Phys. G* **47**(2) (2020) 024001.
- [4] Lu Ren, *JPS Conf. Proc.* **37** (2022) 020309.

Progress on Constraining the Strange Quark Contribution to ...

- [5] S.F. Pate, V. Papavassiliou, J.P. Schaub, D.P. Trujillo, M.V. Ivanov, M.B. Barbaro, C. Giusti, *Phys. Rev. D* **109** (2024) 093001.
- [6] J. Ellis, K.A. Olive, C. Savage, *Phys. Rev. D* **77** (2008) 65026.
- [7] M. Engelhardt, *Phys. Rev. D* **86** (2012) 114510.
- [8] R. Babich, R.C. Brower, M.A. Clark, G.T. Fleming, J.C. Osborn, C. Rebbi, D. Schaich, *Phys. Rev. D* **85** (2012) 054510.
- [9] T. Melson, H.-T. Janka, R. Bollig, F. Hanke, A. Marek, B. Müller, *Astrophys. J. Lett.* **808**(2) (2015) L42.
- [10] T. Gasenzer, O. Nachtmann, M.I. Trappe, *Eur. Phys. J. D* **66** (2012) 113.
- [11] S.F. Pate, *Phys. Rev. Lett.* **92** (2004) 082002.
- [12] J. Liu, R. D. McKeown, M.J. Ramsey-Musolf, *Phys. Rev. C* **76** (2007) 025202.
- [13] D. Androić et al., *Phys. Rev. Lett.* **104** (2010) 012001.
- [14] S. Baunack et al., *Phys. Rev. Lett.* **102** (2009) 151803.
- [15] R.J. Hill, G. Paz, *Phys. Rev. D* **82** (2010) 113005.
- [16] G. Lee, J.R. Arrington, R.J. Hill, *Phys. Rev. D* **92**(1) (2015) 013013.
- [17] A.A. Aguilar-Arevalo et al., *Phys. Rev. D* **82** (2010) 092005.
- [18] A.A. Aguilar-Arevalo et al., *Phys. Rev. D* **91** (2015) 012004.
- [19] R. González-Jiménez, J.A. Caballero, T.W. Donnelly, *Phys. Rev. D* **90**(3) (2014) 033002.